Atmos. Chem. Phys. Discuss., 5, 911–936, 2005
www.atmos-chem-phys.org/acpd/5/911/
SRef-ID: 1680-7375/acpd/2005-5-911
European Geosciences Union

Atmospheric Chemistry and Physics Discussions

Intercomparison of O_3 profiles observed by SCIAMACHY, ground based microwave and FTIR instruments

M. Palm[1], C. v. Savigny[1], T. Warneke[1], V. Velazco[1], J. Notholt[1], K. Künzi[1], J. Burrows[1], and O. Schrems[2]

[1]Institute of Environmental Physics, University of Bremen, PO Box 330440, D-28334 Bremen, Germany
[2]Alfred Wegener Institute for Polar and Marine Research, PO Box 120169, D-27515 Bremerhaven, Germany

Received: 19 April 2004 – Accepted: 10 January 2005 – Published: 18 February 2005

Correspondence to: M. Palm (mathias@iup.physik.uni-bremen.de)

Abstract

Ozone profiles retrieved from limb scattering measurements of the SCIAMACHY instrument based on the satellite ENVISAT are compared to ground based low altitude resolution remote sensors. All profiles are retrieved using optimal estimation. Following the work of Rodgers and Connor (2003) the retrievals of the ground based instruments are simulated using the SCIAMACHY retrieval. The SCIAMACHY results and the results of the ground based microwave radiometer in Bremen and Ny Alesund agree within the expected covariance of the intercomparison. There are not enough coincident measurements of the FTIR instrument in order to allow for a conlusive statistical treatment. However, preliminary intercomparison results are presented.

1. Introduction

The ozone profile is of interest because ozone is one of the most important trace gases in the atmosphere. Ozone is a green house gas and provides shielding from UV radiation. Following the discovery of the ozone hole (Farman et al., 1985) a large effort has been put into understanding the reason for it and to establish a network for monitoring the further development of the ozone layer. Although the emission of human made chemicals (CFCs) has been curbed, the rise in the water vapor content of and the decrease of the temperature in the stratosphere still give reasons of concern about the ozone layer (e.g. Rex et al., 2004).

Remote sounding instruments are used to monitor various atmospheric properties like trace gases from ground or satellite. In the upper stratosphere and above very few if any in-situ measurements are available. All remote sounders are indirect instruments in the sense that they measure a more or less complicated function of the quantity of interest (Rodgers and Connor, 2003). In order to understand and interpret the data taken it is necessary to understand the relationship between the true atmospheric state and the quantity measured. It is also necessary to validate and compare remote sounders on a continuous basis in order to enhance the quality of the measurements and to assess the stability of the combination instrument/retrieval (Rodgers and Connor, 2003).

2. The instruments

2.1. O_3 profiles from SCIAMACHY on Envisat

SCIAMACHY, the Scanning Imaging Absorption spectrometer for Atmospheric CHartographY (Bovensmann et al., 1999) is a novel satellite-borne scientific instrument capable of performing spectroscopic measurements of the chemical composition of the Earth's atmosphere in three different observation geometries: nadir, solar/lunar occultation and limb scattering. SCIAMACHY covers the spectral range from 220 nm to 2380 nm with a spectral resolution varying from 0.2 nm to 1.5 nm depending on wavelength. In limb scattering geometry the instrument line of sight follows a slant path tangentially through the atmosphere. Detected are solar photons that are both (a) scattered along the line of sight into the instrument's field of view, and (b) transmitted from the scattering point to the instrument. The geometrical field of view of SCIAMACHY in limb scattering mode is about 2.8 km vertically and 110 km horizontally. The Earth's limb is viewed in flight direction and scanned from tangent heights of about 0 km up to 100 km in steps of 3.3 km. Furthermore, at every tangent height step an azimuthal (horizontal) scan is performed covering about 960 km at the tangent point. Therefore the limb measurement mode amounts to an averaging over about 1000 km perpendicular to the orbit track. Along the flight track the averaging occurs over a distance of about 400 km.

The stratospheric O_3 profiles used here are derived from SCIAMACHY limb scattering measurements in the Chappuis-bands of O_3. The retrieval algorithm employed is similar to the one described in Flittner et al. (2000), and McPeters et al. (2000), and has also been used for operational data processing of limb scattering observations performed with the Optical Spectrograph and InfraRed Imager System (OSIRIS) (von

Savigny et al., 2003) on the Swedish-led Odin satellite. The retrieval exploits the differential structure of the O_3 cross section between the center (600 nm) and the wings (525 nm and 675 nm) of the Chappuis absorption bands of O_3. A linearized version of optimal estimation (OE) is used together with the radiative transfer model SCIARAYS (Kaiser et al., 2003) to iteratively retrieve stratospheric O_3 concentration profiles. The altitude range from about 15 km up to 40 km can be covered with this technique.

2.2. The millimeter-wave radiometers BreRAM and RAM

The millimeter-wave radiometers RAM (Radiometer for Atmospheric Measurements at Ny Alesund, 78° N, 11° E) and BreRAM (Bremen Radiometer for Atmospheric Measurements at Bremen, 53° N, 8° E) are very similar. Unless specifically noted the following description applies to both.

The instruments are heterodyne millimeter-wave radiometers tuned at the frequency of O_3 lines at 142 GHz (RAM) and 110.836 GHz (BreRAM). Both instruments are operated in total power mode. In order to resolve the spectra the instruments use AOS spectrometers with a bandwidth of about 1 GHz and a effective resolution of 1.3 MHz. The receiver noise temperature is about 3000 K. This enables both instruments to measure a spectrum of the O_3 line every half an hour. Using a special scheme (Wohltmann, 2002) the integration time can be prolonged up to a day in order to enhance signal to noise ratio. Millimeter-wave radiometers are insensitive to meteorological conditions and clouds and do not depend on sun light. They provide therefore the most complete time series of the ozone profile.

The O_3 profile information is retrieved from the spectra using Optimal Estimation Methods (see Sect. 3 and Rodgers, 2000). Information about the vertical ozone distribution between 15 km and 55 km with a height resolution of 15 km at its best can be obtained.

The RAM instrument at Ny Alesund is routinely compared to sonde measurements taken at Ny Alesund. Hence the RAM is validated up to 25 km. Comparisons to LIDAR and satellite measurements have been undertaken (Langer, 1999) with good results:

- Intercomparison with MLS profiles (20–50 km): RAM understimates O_3-vmr. The deviation is smaller than 10%.

- Intercomparison with sonde profiles (18–24 km): RAM overestimates below 20 km and underestimates O_3-vmr above. Deviation smaller than 10%.

- Intercomparison with LIDAR (16–34 km): RAM overestimates the O_3-profile below 20 km and above 30 km. The O_3-profile is underestimated in between. The maximum deviation is 11%.

2.3. The infrared spectrometer FTIR

Solar and lunar absorption measurements using FTIR spectroscopy (Fourier Transform Spectroscopy) have been performed at Ny Alesund since 1992 (Notholt, 1994; Notholt and Schrems, 1994). If weather conditions permit, spectra are recorded at a maximum resolution of 0.005 cm^{-1}. Vertical profiles of ozone were retrieved from these spectra with the SFIT2 algorithm developed at NASA Langley Research Center and the National Institute for Water and Atmospheric Research (New Zealand) (e.g. Rinsland et al., 1998). Based on Pougatchev et al. (1996) and Barret et al. (2002) a spectral interval between 1000 and 1004 cm^{-1} was choosen for the retrieval. Daily launched balloon sondes provide pressure and temperature profiles and the initial vmr-profiles of water up to 30 km. The initial vmr-profiles of ozone are based on ozone sondes launched once or twice a week at Ny Alesund. For all other gases the initial vmr-profiles are based on balloon observations performed in the Arctic at Fairbanks (see Toon et al., 1999). The spectral line parameters were taken from the ATMOS database (Brown et al., 1996).

3. The Optimal Estimation Retrieval

For a detailed discussion of the Optimal Estimation Retrieval (OE) see Rodgers (2000). In this work a brief overview will be given and certain aspects crucial to the understanding of the comparison are discussed. If not noted otherwise the following is based on Rodgers (2000) and Rodgers and Connor (2003).

The retrieval of information about the vertical ozone distribution is mathematically an inverse problem. Detailed understanding of the relation between a given distribution of ozone in the atmosphere and a spectrum measured on the ground or in space is available by the so called forward model $\boldsymbol{F}$. Let $\boldsymbol{x}$ be a given ozone distribution and $\boldsymbol{y}$ a spectrum. A Gaussian distributed error $\boldsymbol{\epsilon}$ with covariance $\mathbf{S}_\epsilon$ will be assumed on the spectrum. Hence $\boldsymbol{y}$ is obtained by

$$\boldsymbol{y} = \boldsymbol{F}(\boldsymbol{x}) + \boldsymbol{\epsilon} = \boldsymbol{F}(\boldsymbol{x}_0) + \frac{\partial \boldsymbol{F}}{\partial \boldsymbol{x}}(\boldsymbol{x} - \boldsymbol{x}_0) + O(\boldsymbol{x}^2) + \boldsymbol{\epsilon} \quad (1)$$

which is called the forward problem with the weighting function matrix $\mathbf{K}=\frac{\partial \boldsymbol{F}}{\partial \boldsymbol{x}}$. Using Bayes law the following relationship for the inverse model (for the detailed discussion please see Rodgers, 2000) is found. Let $\boldsymbol{x}_a$ be the a priori profile of O_3 and $\mathbf{S}_a$ the covariance matrix of $\boldsymbol{x}_a$. Let $P(\boldsymbol{x}|\boldsymbol{y})$ denote the probability of getting a ozone distribution $\boldsymbol{x}$ given a spectrum $\boldsymbol{y}$. The probability distribution $P(\boldsymbol{x}|\boldsymbol{y})$ can be written as:

$$P(\boldsymbol{x}|\boldsymbol{y}) = \exp(-(\boldsymbol{F}(\boldsymbol{x}) - \boldsymbol{y})^T \mathbf{S}_\epsilon^{-1} (\boldsymbol{F}(\boldsymbol{x}) - \boldsymbol{y})) \exp(-(\boldsymbol{x}_a - \boldsymbol{x}) \mathbf{S}_a^{-1} (\boldsymbol{x}_a - \boldsymbol{x})) \quad (2)$$

In OE the solution, the otimal profile $\hat{\boldsymbol{x}}$, is found by

$$\hat{\boldsymbol{x}} = \boldsymbol{x}_a + \mathbf{S}_a \mathbf{K}^T (\mathbf{K}\mathbf{S}_a\mathbf{K}^T + \mathbf{S}_\epsilon)^{-1} (\boldsymbol{y} - \mathbf{K}\boldsymbol{x}_a). \quad (3)$$

In the case of a weakly non-linear forward model the solution can be found by an iterative algorithm like the Levenberg-Marquardt-Algorithm. By defining

$$\mathbf{D} = \mathbf{S}_a \mathbf{K}^T (\mathbf{K}\mathbf{S}_a\mathbf{K}^T + \mathbf{S}_\epsilon)^{-1} \quad (4)$$

Eq. (3) can be written as

$$\hat{\boldsymbol{x}} = \boldsymbol{x}_a + \mathbf{D}(\boldsymbol{y} - \mathbf{K}\boldsymbol{x}_a) \tag{5}$$

and noting that $\boldsymbol{y}=\mathbf{K}\boldsymbol{x}_{True}$ (the error $\boldsymbol{\epsilon}$ has been omitted), the so called instrument model is

$$\hat{\boldsymbol{x}} = \boldsymbol{x}_a + \mathbf{D}(\mathbf{K}\boldsymbol{x}_{True} - \mathbf{K}\boldsymbol{x}_a) = \boldsymbol{x}_a + \mathbf{A}(\boldsymbol{x}_{True} - \boldsymbol{x}_a). \tag{6}$$

Equation (6) relates the unknown true profile $\boldsymbol{x}_{True}$ to the profile retrieved. The matrix $\mathbf{A}$ is called the resolution kernel matrix and can also be written by

$$\mathbf{A} = \frac{\partial \hat{\boldsymbol{x}}}{\partial \boldsymbol{x}_{True}}. \tag{7}$$

The resolution kernel matrix $\mathbf{A}$ contains information about the sensitivity of the instrument/retrieval to changes in the true profile.

3.1. Intercomparison of indirect measurements

Assume two retrievals 1 and 2 with respect to the a priori $\boldsymbol{x}_a$ and $\boldsymbol{x}_c$, respectively. The direct difference $\boldsymbol{\delta}_x$ of two profiles $\hat{\boldsymbol{x}}_1$ and $\hat{\boldsymbol{x}}_2$ is

$$\begin{aligned}\boldsymbol{\delta}_x = \hat{\boldsymbol{x}}_1 - \hat{\boldsymbol{x}}_2 &= \boldsymbol{x}_a + \mathbf{A}_1(\boldsymbol{x}_{True} - \boldsymbol{x}_a) \\ &- (\boldsymbol{x}_c + \mathbf{A}_2(\boldsymbol{x}_{True} - \boldsymbol{x}_c)) + \boldsymbol{\epsilon}_1 - \boldsymbol{\epsilon}_2 \\ &= (\mathbf{A}_1 - \mathbf{A}_2)(\boldsymbol{x}_{True} - \boldsymbol{x}_c) \\ &- (\mathbf{A}_1 - \mathbf{I})(\boldsymbol{x}_a - \boldsymbol{x}_c) + \boldsymbol{\epsilon}_1 - \boldsymbol{\epsilon}_2.\end{aligned} \tag{8}$$

The term $(\mathbf{I}-\mathbf{A})(\boldsymbol{x}_a-\boldsymbol{x}_c)$ contains the difference of the a priori profiles of the retrievals. For simplicity all profiles have been transformed to be with respect to the a priori profile $\boldsymbol{x}_c$. This has been done by adding the term $(\mathbf{A}_1-\mathbf{I})(\boldsymbol{x}_a-\boldsymbol{x}_c)$ to the retrieved profile in question. Let $\mathbf{S}_{x_1}$, $\mathbf{S}_{x_2}$ be the error covariances of retrieval 1 and 2, respectively. The expected error covariance $\mathbf{S}_\delta$ of the difference of the profiles (Eq. 8) is

$$\mathbf{S}_\delta = (\mathbf{A}_1 - \mathbf{A}_2)\mathbf{S}_c(\mathbf{A}_1 - \mathbf{A}_2)^T + \mathbf{S}_{x_1} + \mathbf{S}_{x_2}. \tag{9}$$

The expected variance of the profile difference may be quite large (Fig. 1 for an example). Following Rodgers and Connor (2003) another comparison method, retrieval simulation, leads to much smaller expected variances in the profile differences.

3.2. Simulating one retrieval with another

Again it is assumed that both profiles $\hat{\boldsymbol{x}}_1$ and $\hat{\boldsymbol{x}}_2$ are with respect to the same a priori profile $\boldsymbol{x}_c$. The retrieval 1 is simulated using retrieval 2 by:

$$\hat{\boldsymbol{x}}_{12} = \boldsymbol{x}_c + \boldsymbol{A}_1(\hat{\boldsymbol{x}}_2 - \boldsymbol{x}_c). \quad (10)$$

The difference of the profiles is

$$\boldsymbol{\delta}_{12} = \boldsymbol{x}_1 - \boldsymbol{x}_{12} = (\mathbf{A}_1 - \mathbf{A}_1\mathbf{A}_2)(\boldsymbol{x} - \boldsymbol{x}_c) + \boldsymbol{\epsilon}_1 - \boldsymbol{\epsilon}_2 \quad (11)$$

and the covariance of the difference is found by

$$\mathbf{S}_{12} = (\mathbf{A}_1 - \mathbf{A}_1\mathbf{A}_2)\mathbf{S}_c(\mathbf{A}_1 - \mathbf{A}_1\mathbf{A}_2)^T + \mathbf{S}_1 + \mathbf{A}_1\mathbf{S}_2\mathbf{A}_1^T. \quad (12)$$

The expected variances of the ground based retrievals simulated by the SCIAMACHY retrieval are shown in Fig. 1. For the intercomparison using simulated retrievals the expected standard deviation is smaller than for direct intercomparison. In fact it is only little larger than the expected standard deviation for the BreRAM profile.

4. Results

4.1. Assumptions and procedure of the comparison

The most important difference of the SCIAMACHY instrument on the one hand and all other, ground based, instruments on the other hand is the measuring geometry. While SCIAMACHY measurements are integrated over a large area (the SCIAMACHY pixel is about 1000 km×400 km) the ground based instruments integrate over an area of less than 100 km×100 km depending on the viewing angle.

Measurements are compared if the location of the ground based instrument is within the SCIAMACHY pixel plus 500 km. Also, the time difference is required to be less than 2 h. Care has been taken in order to measure comparable air masses. There are several options to consider:

1. The total ozone column is compared. A paper by Lamsal et al. (2003) indicates that the ozone profile for a given latitude and season approximately scales with the total O_3-column. The O_3 column above the site of the ground based instruments m_G is required to be comparable to the mean ozone O_3 column m_S within the SCIAMACHY pixel, i.e. $|2(m_G - m_S)/(m_G + m_S)| < m_0$ (see Table 1). The variation within the SCIAMACHY pixels is required to be smaller than a maximum d_0 in order to exclude pixels where e.g. filaments disturb the homogeneity of the atmosphere. m_0 and d_0 are chosen differently for the instruments in order to get a good balance between the number of coincident measurements and the quality of the profiles compared. The total ozone columns were measured by the TOMS satellite but will be provided by SCIAMACHY itself in future.

2. The potential vorticity (PV) is calculated in order to ensure that the measurements are completely either inside or outside the polar vortex. The same PV of either larger than 40 PVU (potential vorticity units; inside the vortex) or smaller than 30 PVU (outside the vortex) is required for both measurement areas. All coincident measurements in 2003 above Ny Alesund were outside the vortex.

The retrieved ozone profiles have been processed as follows:

1. vmrs are calculated from the concentration profiles provided by SCIAMACHY using ECMWF ERA-40 temperature and pressure profiles,

2. the profiles are transformed to a common a priori (taken from the climatology used by the SCIAMACHY retrieval) $\boldsymbol{x}_c$ and

3. the retrievals of the ground based instruments are simulated using the SCIAMACHY retrieved profiles by

$$\hat{\boldsymbol{x}}_{SIM} = \boldsymbol{x}_c + \mathbf{A}_G(\hat{\boldsymbol{x}}_S - \boldsymbol{x}_c), \tag{13}$$

where the index G denotes a quantity derived from the measurements of one of the ground based instruments BreRAM, RAM and FTIR. The index S denotes a quantity derived from the SCIAMACHY measurement.

In this work profiles are compared on a profile by profile basis. The relative mean deviation Δ_x of N profiles is

$$\Delta_x = \sum_{i=1}^{N} \frac{2 * (\hat{x}^i_G - \hat{x}^i_{SIM})}{\hat{x}^i_G + \hat{x}^i_{SIM}}. \tag{14}$$

In a second comparison it has been examined if the retrieved maximum of the O_3-vmr is at the same altitude in the compared retrievals. This test is very sensitive to differences in the a priori profile and differences in the height resolution of the instruments.

4.2. Comparison results SCIAMACHY – BreRAM

Between August 2002 and August 2003 64 collocations were found. After checking for the total O_3 columns 30 coincident measurements were discarded.[1] The profiles in Fig. 2 show a very good agreement of the shapes of the retrieved O_3 profiles. The relative mean of the difference (Fig. 3) also shows a good agreement between the BreRAM and the SCIAMACHY profile. The relative mean deviation is smaller than 10% and is within the expected standard deviation $\mathbf{S}_{12}$ of the comparison. The altitude of the

[1] Increasing the number of coincident measurements by trajectory hunting methods (e.g. Danilin et al., 2002) is not possible because of the altitude resolution of the ground based instruments (see also Langer, 1999).

maximum vmr is found in 75% of the retrievals (see Fig. 4). However, the SCIAMACHY retrieval tends to underestimate the vmr apart from the range 15–20 km.

It must be mentioned that the SCIAMACHY limb observations suffered from inaccuate pointing for all the measurements used in this study. Tangent height offsets of up to 3 km were detected. The limb pointing is very accurate immiately after the daily updates of the on-board orbit model. After these updates, the pointing slowly deviates from nominal pointing until the next update occurs. As a first order pointing correction a constant tangent height offset of 1.5 km was subtracted from the tangent heights prior to the inversion procedure. This implies, that tangent height offsets of up to 1.5 km have to be expected. These offsets basically lead to a retrieved O_3 profile that is shifted by the tangent height error (von Savigny et al., 2004).

4.3. Comparison results SCIAMACHY-RAM

Between August 2002 and August 2003 95 collocations have been found. By applying the checks for the total O_3 column 60 coincident measurements were discarded.

The profiles in Fig. 5 show very good agreement in the shape of the profiles and the vmr retrieved. The relative mean deviation is smaller than 15%, i.e. somewhat larger than for the SCIAMACHY-BreRAM comparison. Above 35 km SCIAMACHY retrieves vmr values higher than the RAM. The altitude of the maximum vmr is found in most of the cases.

4.4. Intercomparison results SCIAMACHY-FTIR

In contrast to microwave spectroscopy solar absorption FTIR-spectra can only be obtained under clear sky conditions. This results in a lower number of coincident measurements. For this reson the conditions on the O_3-column have been relaxed (Table 1).

From the initial 28 concident measurements 6 were discarded. The remaing coincident measurements are distributed over two days with 20 of the measurements on 1

August 2003. Due to the low number of coincident measurements the statistical treatment presented in this study is not yet conclusive. However it is interesting to look at the preliminary results.

The general shape of the O_3 profiles agrees but the values of the retrieved vmr below 20 km differs significantly. From 20 km up to 50 km the relative mean deviation is still quite high. The height of the maximum vmr is rarely found (Fig. 10).

5. Conclusions

Comparisons of the high altitude resolution remote sounder SCIAMACHY with two ground based millimeter-wave sounders and a ground based FTIR sounder are shown.

The comparability is ensured by constraints on the SCIAMACHY pixel in terms of the total ozone column and the potential vorticity. The profiles retrieved from the SCIAMACHY measurements and the millimeter wave measurements agree in shape as well as in height of the maximum vmr. The differences in the retrieved vmr are in the range of the expected standard deviation of the comparison except above 35 km in case of the RAM. The coincident measurements with the FTIR instrument are very sparse so that it is difficult to compare them properly. The general shape of the profile is found but the altitude of the maximum as well as the retrieved vmr profiles differ.

The statistical basis for the intercomparison of this study is still quite small. However, the statistical basis is expected to improve with the lifetime of the SCIAMACHY instrument. Newer millimeter wave instruments like RAMAS on Greenland (Golchert et al., 2004) will contribute more coincident measurements and improve the quality of the comparison because of their better altitude resolution (expected 10 km over a range of 20 to 45 km).

Acknowledgements. We would like the Alfred Wegener Institute Bremerhaven for providing the infrastructure to carry out millimeter-wave and FTIR measurements at Ny Alesund, Spitsbergen. We also thank the various technicians and other personnel at the research station in Ny Alesund and in Bremen for their support.

For providing the data of total O_3 columns we thank the NASA Goddard Space Flight Center.

This work has been funded by the DLR.

References

Barret, B., Mazière, M. D., and Demoulin, P.: Retrieval and characterization of ozone profiles from solar infrared spectra at the Jungfraujoch, J. Geophys. Res., 107(D24), 4788, doi:10.1029/2001JD001298, 2002. 915

Bovensmann, H., Burrows, J. P., Buchwitz, M., Frerick, J., Noël, S., Rozanov, V. V., Chance, K. V., and Goede, A. P. G.: SCIAMACHY: Mission Objectives and Measurement Modes, J. Atmos. Sci., 56, 127–150, 1999. 913

Brown, L., Gunson, M., Toth, R., Irion, F., Rinsland, C., and Goldman, A.: The 1995 atmospheric trace molecule spectroscopy (ATMOS) linelist, Appl. Opt., 35, 2828–2848, 1996. 915

Danilin, M., Ko, M., Froidevaux, L., Santee, M., Lyjak, L., Bevilacqua, R., Zawodny, J., Sasano, Y., Irie, H., Kondo, Y., Russel III, J., Scott, C., and Read, W.: Trajectory hunting as an effective technique to validate multiplatform measurements: Analysis of the MLS, HALOE, SAGE-II, ILAS, and POAM data October-November 1996, J. Geophys. Res., 107(D20), 4420, doi:10.1029/2001JD002012, 2002. 920

Farman, J., Gardiner, B., and Shanklin, J.: Large losses of total ozone in Antarctica reveal seasonal ClOx/NOx interaction, Nature, 315, 207–210, 1985. 912

Flittner, D. E., Bhartia, P. K., and Herman, B. M.: O_3 profiles retrieved from limb scatter measurements, Geophys. Res. Lett., 27, 2061–2064, doi:10.1029/1999GL011343, 2000. 913

Golchert, S., Buschmann, N., Kleindienst, A., Palm, M., Künzi, K., Notholt, J., de la Nöe, J., Schneider, N., Sorensen, H., Gross, A., and Chipperfield, M.: Comissioning of the new Ground-Based Microwave Radiometer RAMAS at Summit, Greenland, Poster presentation at the Microrad04 conference in Rom, Italy, http://www.ram.uni-bremen.de/pdf_poster/poster_rome-microrad04_ramas.pdf, 2004. 922

Kaiser, J. W., Rozanov, V. V., and Burrows, J. P.: Fast weighting functions for retrievals from limb scattering measurements, JQSRT, 77, 273–283, 2003. 914

Lamsal, L., Weber, M., Tellmann, S., and Burrows, J.: Ozone column classified climatology of ozone and temperature profiles based on ozonesonde and satellite data, J. Geophys. Res., 109, doi:10.1029/2004JD004680, 2004. 919

Langer, J.: Measurements of Arctic stratospheric ozone: Comparison of ozone-measurements at Ny-Alesund, Spitsbergen, in 1997 and 1998, PhD thesis, University of Bremen, in German, 1999. 915, 920

McPeters, R. D., Janz, S. J., Hilsenrath, E., Brown, T. L., Flittner, D., and Heath, D.: The retrieval of O_3 profiles from limb scatter measurements: Results from the Shuttle Ozone Limb Sounding Experiment, Geophys. Res. Lett., 27(17), 2597–2600, doi:10.1029/1999GL011342, 2000. 913

Notholt, J.: The moon as light source for FTIR measurements of stratospheric trace gases during the polar night: Application for HNO3 in the Arctic, J. Geophys. Res., 99, 3607–3614, 1994. 915

Notholt, J. and Schrems, O.: Ground-based FTIR measurements of vertical column densities of several trace gases above Spitzbergen, Geophys. Res. Lett., 21, 1355–1358, 1994. 915

Pougatchev, N. S., Connor, B. J., and Rinsland, C. P.: Validation of ozone profile retrievals from ground-based solar spectra, Geophys. Res. Lett., 23(13), 1637–1640, 1996. 915

Rex, M., Salawitch, R., von der Gathen, J. P., Harris, N., Chipperfield, M., and Naujokat, B.: Arctic ozone loss and climate change, Geophys. Res. Lett., 31, L04 116, doi:10.1029/2003GL018844, 2004. 912

Rinsland, C. P., Jones, N. B., Connor, B. J., et al.: Northern and southern hemisphere ground-based infrared spectroscopic measurements of tropospheric carbon monoxide and ethane, J. Geophys. Res., 103(D21), 28 197–28 217, 1998. 915

Rodgers, C. D.: Inverse methodes for atmospheric sounding, vol. 2 of Series on Atmospheric, Oceanic and Planetary Physics, World Scientific, 2000. 914, 916

Rodgers, C. D. and Connor, B. J.: Intercomparison of remote sounding instruments, J. Geophys. Res., 108, doi:10.1029/2002JD002299, 2003. 912, 913, 916, 918

Toon, G. C., Blavier, F.-F., Sen, B., Salawitch, R. I., Ostermann, G. B., Notholt, J., Rex, M., McElroy, G. T., and Russell III, M.: Ground-based observations of Arctic O3 loss during spring and summer 1997, J. Geophys. Res., 104, 26 497–26 510, 1999. 915

von Savigny, C., Haley, C. S., Sioris, C. E., et al.: Stratospheric Ozone Profiles retrieved from Limb Scattered Sunlight Radiance Spectra Measured by the OSIRIS Instrument on the Odin Satellite, Geophys. Res. Lett., 30, doi:10.1029/2002GL016401, 2003. 913

von Savigny, C., Rozanov, A., Bovensmann, K.-U., Noël, S., Rozanov, V. V., Sinnhuber, B. M., Weber, M., Burrows, J. P., and Kaiser, J. W.: The ozone hole break up in September 2002 as seen by SCIAMACHY on ENVISAT, J. Atmos. Sci., in press, 2004. 921

Wohltmann, I.: Ozone depletion, chlorine activation and water vapour observed in Spitsbergen, PhD thesis, Universität Bremen, 2002. 914

ACPD
5, 911–936, 2005

Intercomparison of O_3 profiles

M. Palm et al.

Table 1. Limits m_0 and d_0 for the intercomparison of SCIAMACHY with different ground based instruments.

	m_0	d_0
BreRAM	5%	10%
RAM	5%	10%
FTIR	20%	20%

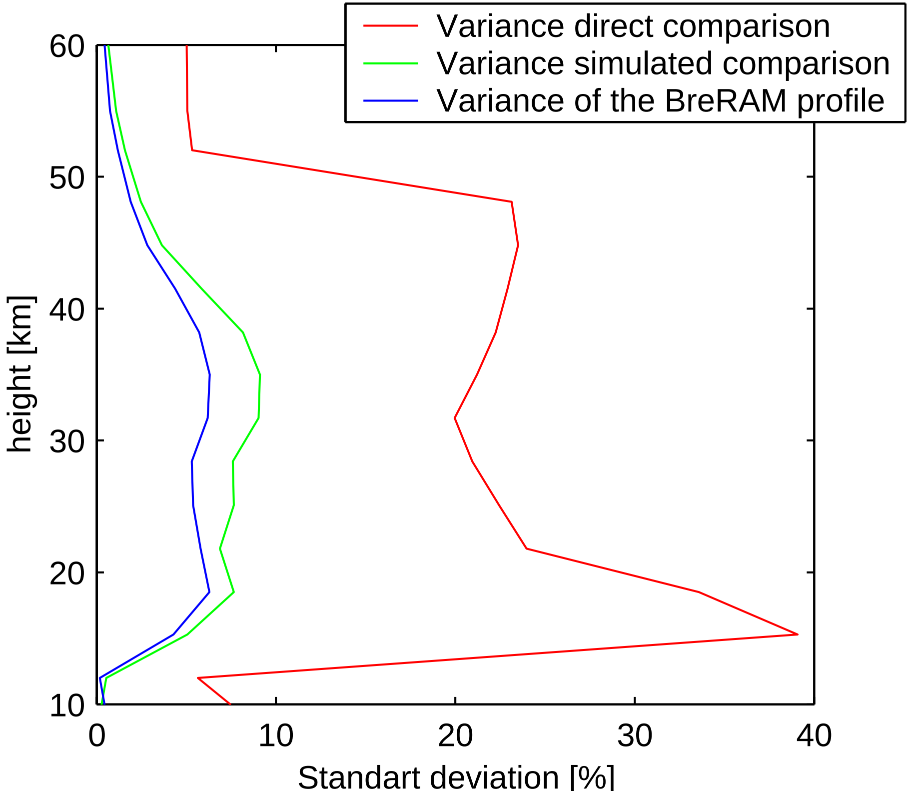

Fig. 1. Expected standard deviations of the direct intercomparison of the BreRAM-SCIAMACHY profiles, the intercomparison of the BreRAM profile with a simulated profile (using the SCIAMACHY profile as $\boldsymbol{x}_2$ (Eq. 10). For comparison the expected standard deviation of the BreRAM profile has been plotted. The results are the comparable for all ground based instruments considered in this work.

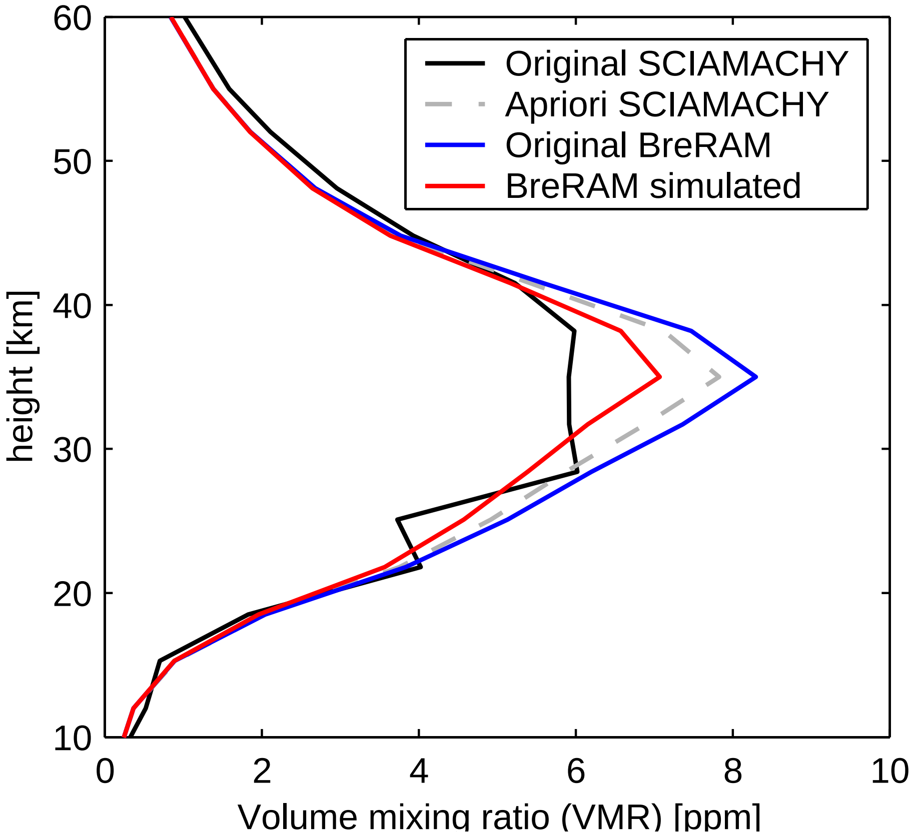

Fig. 2. Example profiles retrieved by SCIAMACHY (black), the same convolved with $\mathbf{A}_{BreRAM}$ (red) and the BreRAM vmr profile (blue) of Ozone the thin grey line is the a priori profile used in the SCIAMACHY retrieval.

ACPD
5, 911–936, 2005

Intercomparison of O_3 profiles

M. Palm et al.

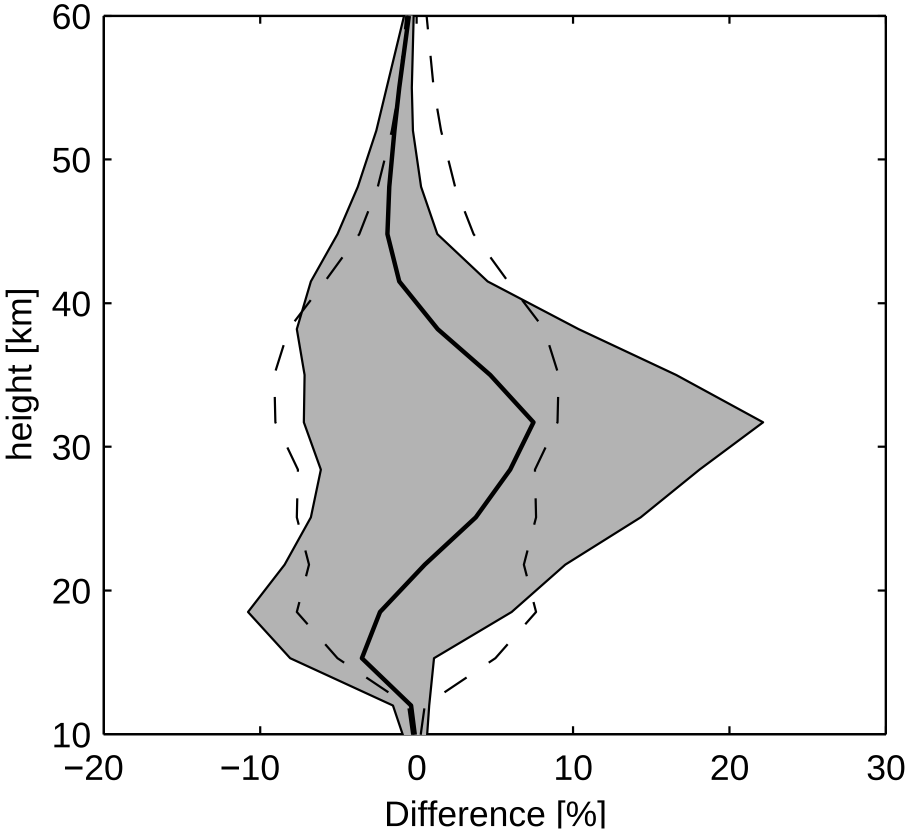

Fig. 3. Relative mean difference Δ_x (see Formula 14) BreRAM to SCIAMACHY. The shaded area is the standard deviation of Δ_x and the dashed line denotes the standard deviation of the comparison $\mathbf{S}_{12}$.

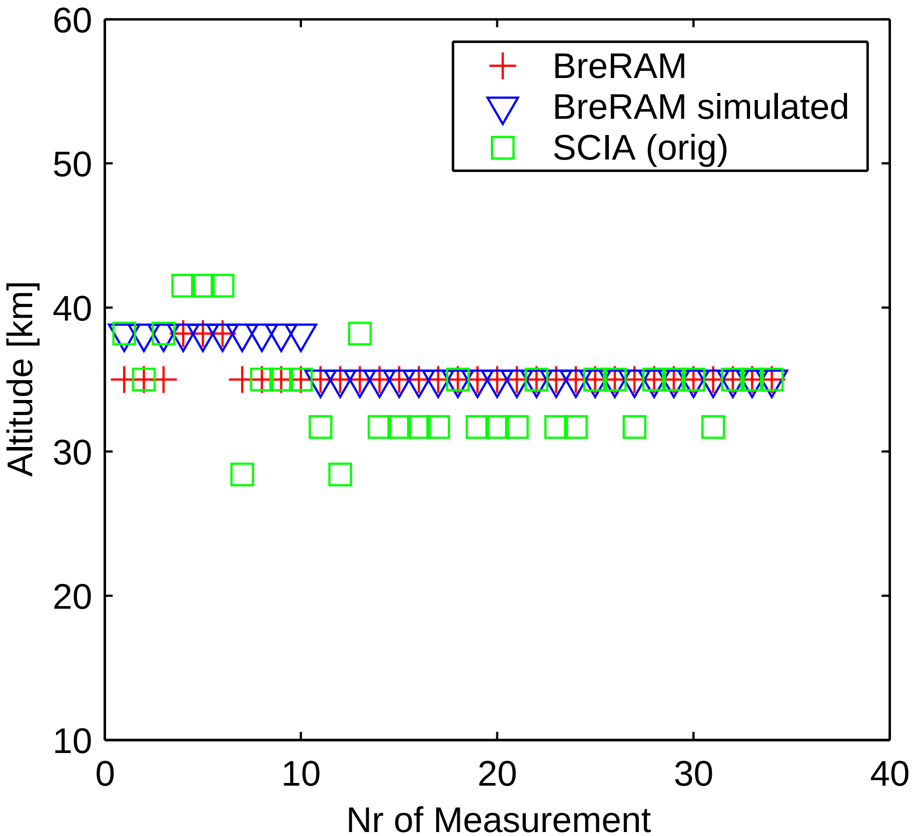

Fig. 4. Altitudes of the maximum of the retrieved volume mixing ratio.

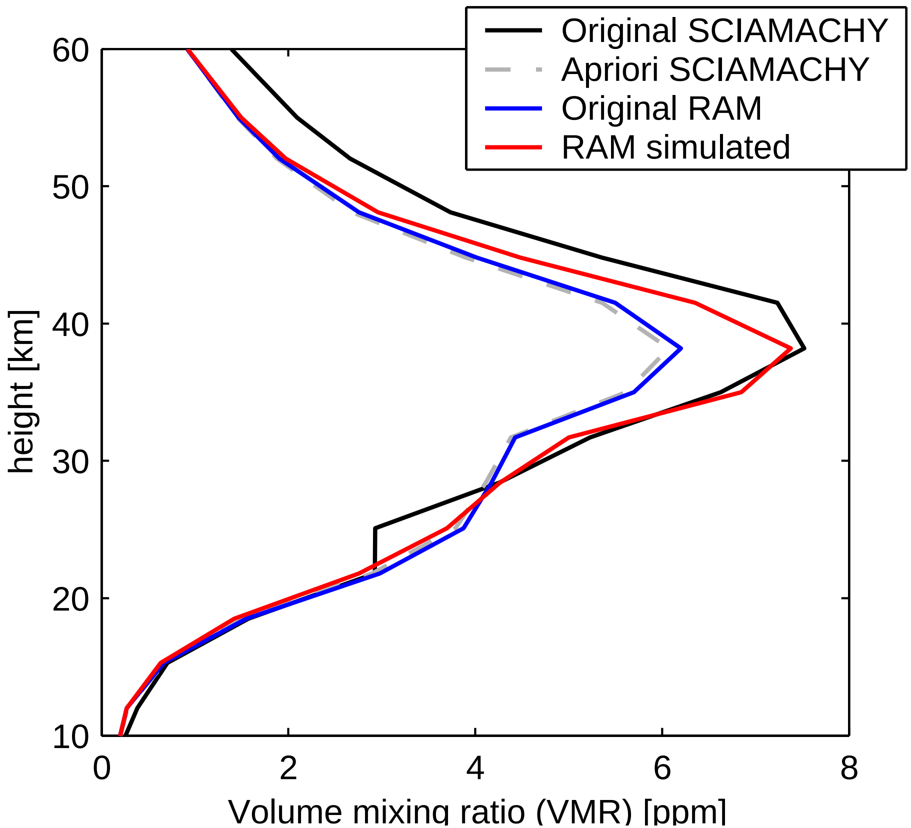

Fig. 5. Example profiles retrieved by SCIAMACHY (black), the same convolved with $\mathbf{A}_{RAM}$ (red) and the RAM vmr profile (blue) of Ozone, the thin grey line is the a priori profile used by the SCIAMACHY retrieval.

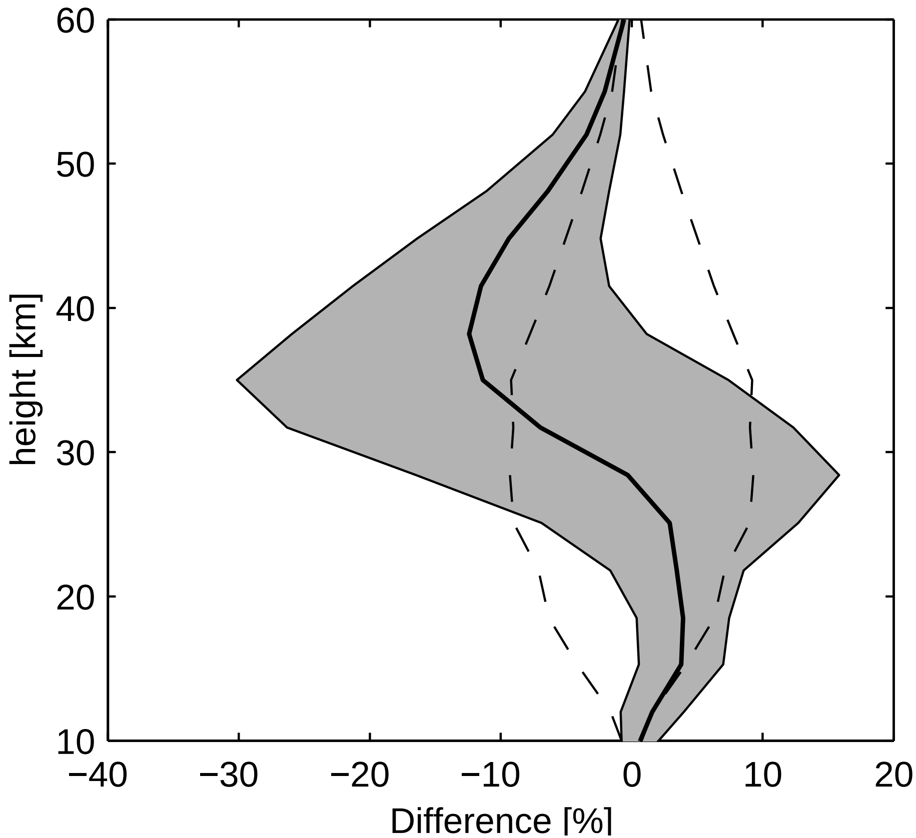

Fig. 6. Relative mean difference Δ_x (see Formula 14) RAM to SCIAMACHY. The shaded area is the standard deviation of Δ_x and the dashed line denotes the standard deviation of the comparison $\mathbf{S}_{12}$.

ACPD
5, 911–936, 2005

Title Page
Abstract | Introduction
Conclusions | References
Tables | Figures
◀| |▶
◀ ▶
Back | Close
Full Screen / Esc
Print Version
Interactive Discussion
EGU

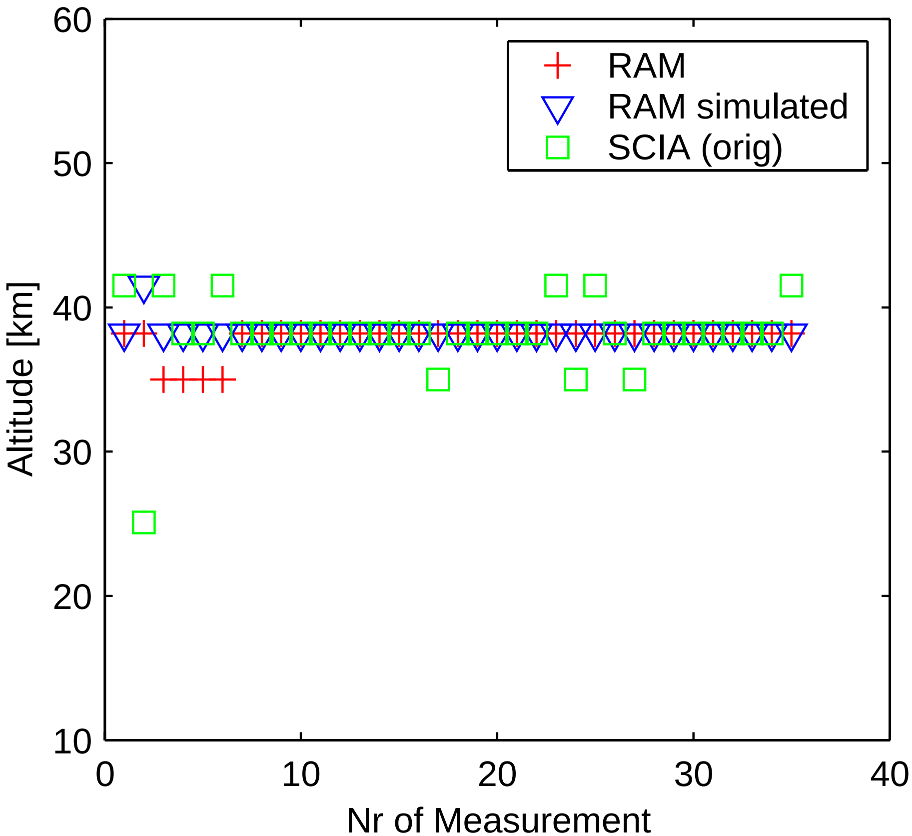

Fig. 7. Altitudes of the maximum of the retrieved volume mixing ratio.

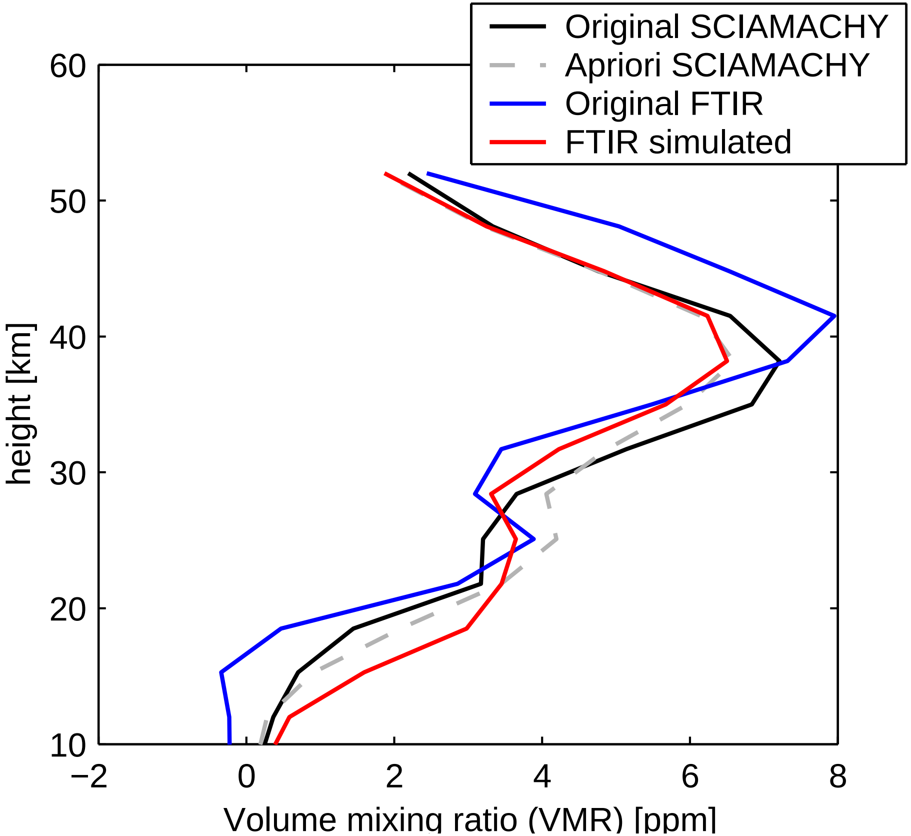

Fig. 8. Example profiles retrieved by SCIAMACHY (black), the same convolved with $\mathbf{A}_{FTIR}$ (red) and the FTIR vmr profile (blue) of Ozone, the thin grey line is the a priori profile used by the SCIAMACHY retrieval.

ACPD
5, 911–936, 2005

Title Page
Abstract | Introduction
Conclusions | References
Tables | Figures
◂ | ▸
Back | Close
Full Screen / Esc
Print Version
Interactive Discussion

EGU

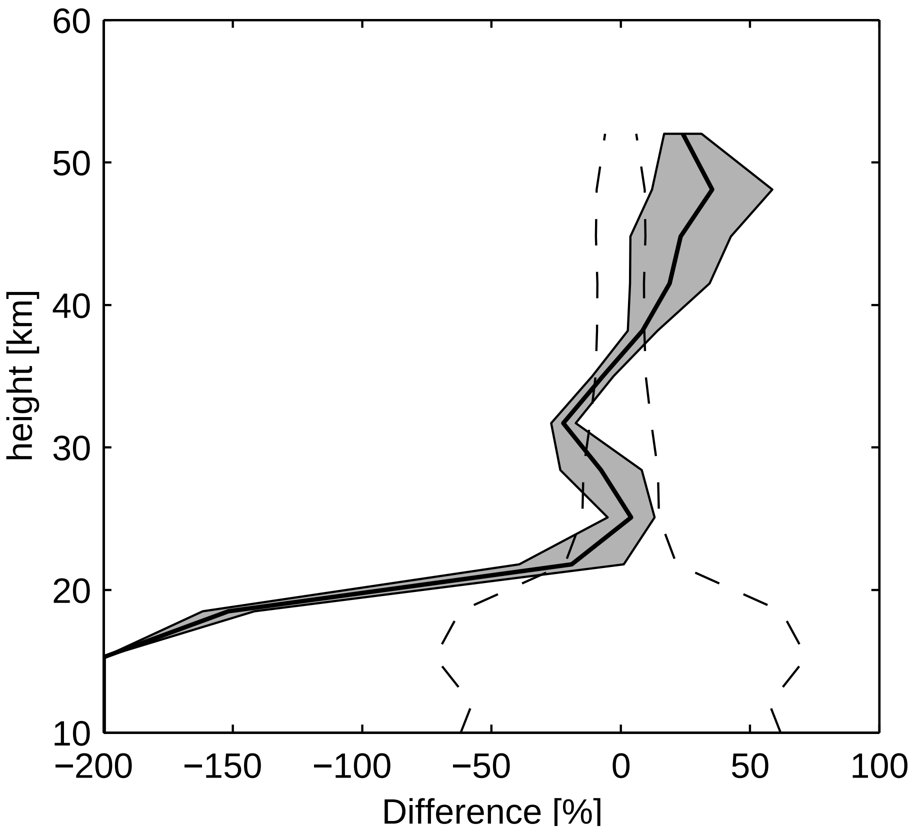

Fig. 9. Relative mean difference Δ_x (see Formula 14) FTIR to SCIAMACHY. The shaded area is the standard deviation of Δ_x and the dashed line denotes the standard deviation of the comparison $\mathbf{S}_{12}$.

ACPD
5, 911–936, 2005

Title Page
Abstract | Introduction
Conclusions | References
Tables | Figures
◀◀ | ▶▶
◀ | ▶
Back | Close
Full Screen / Esc
Print Version
Interactive Discussion

EGU

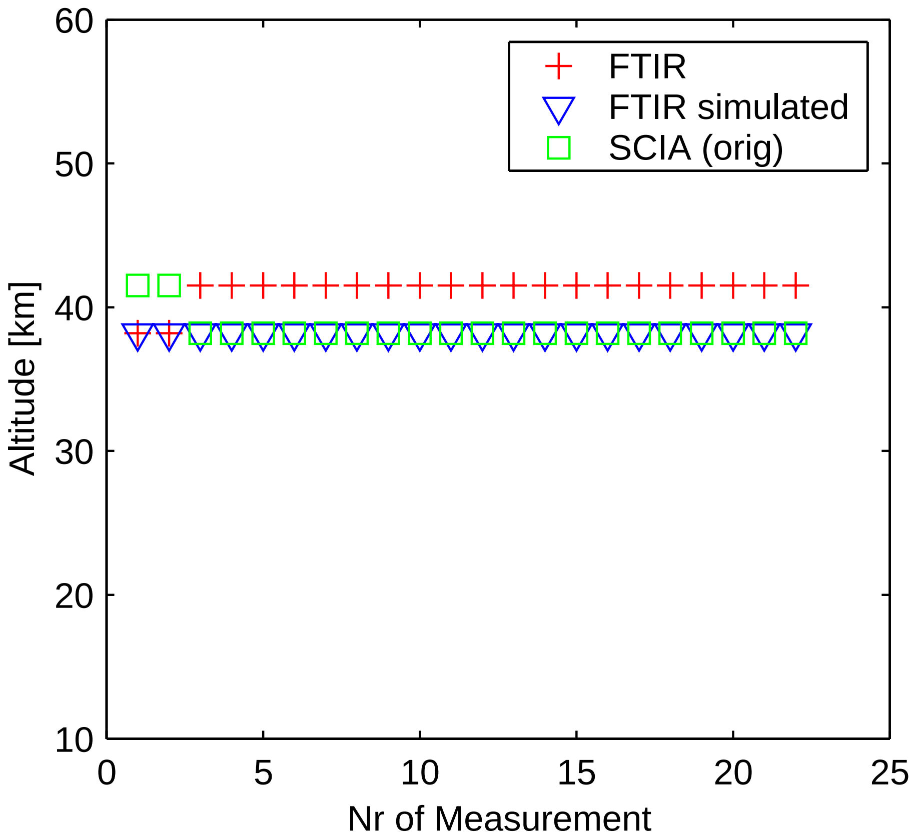

Fig. 10. Altitudes of the maximum of the retrieved volume mixing ratio.